J Mater Sci (2011) 46:2495–2502
DOI 10.1007/s10853-010-5098-8

Non-linear viscoelasticity of vapor grown carbon nanofiber/polystyrene composites

Li Zhao · Hongmei Yang · Yihu Song · Yujie Zhou · Guo-hua Hu · Qiang Zheng

Received: 18 April 2010 / Accepted: 19 November 2010 / Published online: 14 December 2010

Abstract The strain (γ) dependences of viscoelasticity and electrical resistance (R) of vapor grown carbon nanofiber (VGCF)/polystyrene (PS) composites have been studied using simultaneous measurement technique. The composites containing at least 4 vol.% VGCF present two regions of strain softening at $\gamma < 10\%$ and $\gamma > 30\%$, respectively. Using strain amplification factor introduced by hydrodynamic effects as vertical and horizontal shifting factors, the curves of dynamic storage modulus (G') and loss modulus (G'') as a function of γ for the composites can be superposed, respectively, on those for the pure matrix at $\gamma \geq 30\%$. Significant deflection from the master curves can be observed at $\gamma < 30\%$. R tested as a function of γ provides direct evidences for breakdown of filler–filler interactions even by a small strain perturbation. It is suggested that breakdown of filler–filler interactions plays a vital role in strain softening at small strains, whereas the matrix provides the main contribution to strain softening at large strains. Dynamic moduli $G'_{f,(0.1\%,\varphi)}$ and $G''_{f,(0.1\%,\varphi)}$ of the filler phase at volume fraction φ at 0.1% strain are used to account for the viscoelastic contribution of the initial filler structure. Ratios of dynamic moduli of the filler phase to the composite at 0.1% strain, $G'_{f,0.1\%}/G'_{c,0.1\%}$ and $G''_{f,0.1\%}/G''_{c,0.1\%}$, exhibit percolation-like transition as a function of φ, which is in consistence with the electric percolation transition.

L. Zhao · H. Yang · Y. Song · Y. Zhou · Q. Zheng (✉)
Department of Polymer Science and Engineering, Zhejiang University, Hangzhou 310027, People's Republic of China
e-mail: zhengqiang@zjuem.zju.edu.cn

L. Zhao · H. Yang · Y. Song · Y. Zhou · Q. Zheng
Key Laboratory of Macromolecular Synthesis and Functionalization, Ministry of Education, Hangzhou 310027, People's Republic of China

G. Hu
Laboratory of Chemical Engineering Sciences, Nancy Universite, CNRS-ENSIC-INPL, 1 rue Grandville, BP 20451, 54001 Nancy Cedex, France

Introduction

Incorporating functional fillers is a popular approach to modify polymers [1–5], and the filler reinforcement is typically reflected in the increased storage modulus (G') and viscosity beyond those of the matrix. Filled polymers generally exhibit nonlinear viscoelasticity under strains (γ), which is often referred to Payne effect [6–8].

Payne effect appearing as G' decay with increasing γ in filled polymers has been related to filler network breakdown [8–11], filler deagglomeration [12, 13], polymer–filler debonding from the filler surface [14], and strain softening of the polymer shell surrounding fillers [15]. However, underlying mechanisms for Payne effect of filled polymers are not yet clarified. For instance, the concepts of filler deagglomeration and network breakdown do not consider the contributions from the matrix and the filler–polymer interactions, and they could not explain Payne effect in the case of filler content below percolation threshold. The nonlinear viscoelasticity observed in many systems always differ in strength and type of interparticle force, shape, and average size of fillers, as well as the nature of matrix [11–15], which have not been included in phenomenological models.

In recent years, conductive nanofiller/polymer composites have attracted researchers' attention because of their excellent multifunctional properties in comparison with conventional conductive polymer composites [16–20].

There exist a lot of available nanofillers [21–27], among which vapor grown carbon nanofiber (VGCF) is an excellent conductive nanofiller [20]. Linear viscoelasticity has been applied to assess the state of dispersion of fillers in the melt. Strain-sweep tests are generally performed for determining linear viscoelastic regime. Few works concerning phenomena of nonlinear viscoelasticity have been reported to VGCF filled polymers while exploration of the origin of Payne effect is usually ignored [28, 29]. Schaefer et al. [30] observed strain softening even at $\gamma = 0.4\%$ in 2 wt% VGCF filled thermoplastic polyurethane elastomer (TPU). In comparison, the phenomenon that linear region disappears has not been observed in carbon black (CB) filled TPU. Schaefer et al. ascribed the strain softening in VGCF/TPU to the slippage of the deformed filler cluster in the matrix. However, this idea ignores the filler deagglomeration that occurs inevitably and requires a further study in detail. In fact, strain softening in filled polymers is inextricably linked with disruption of the filler–filler and the filler–matrix interactions. Breakdown of filler–filler contacts and chain debonding from the filler phase should always entangle with each other in conventional rheological measurements.

Simultaneous measurements of rheological and conductive properties have been used to study the structure and properties of filled natural rubber [7] or vulcanizates [31] as well as electric conduction behaviors of an electrorheological fluid suspension [32]. Our group has put forward a novel simultaneous measurement of electric resistance (R) and rheological parameters for conductive polymer composites [10, 33, 34]. In this article, we focus our attention on the nonlinear viscoelasticity of VGCF filled polystyrene (PS) by simultaneous measurement technology applied in strain sweep mode. Here, the strain-dependent R is pursued to evaluate the variation of filler–filler interactions during strain softening due to shear action. We aim to gain the mechanisms for nonlinear viscoelasticity especially the origin of strain softening in low strain region for VGCF filled composites.

Experimental

Materials

Polystyrene (PS, SGM-085) with density of 1.04 g/m^3, number average molecular weight of approximate 84.9 kg/mol, and polydispersity index of 2.3 was supplied by Certene, USA. Highly crystalline carbon nanofiber (VGCF, VGCF-H) synthesized by the vapor-phase method with average diameter of 150 nm, length of 10 μm, and electric resistivity of $1 \times 10^{-4}\ \Omega$ cm was supplied by Showa Denko Co. Ltd., Japan. Styrene–maleic anhydride copolymer (SMA) with number average molecular weight of 11 kg/mol and maleic anhydride content of 18.5 wt% was made in our laboratory. Antioxdant (B215) with relative molecular weight of 647 and melting temperature of 180–185 °C was supplied by Ciba-Geigy Co., Japan.

Samples preparation

After being dried at 80 °C for 24 h, VGCF and PS matrix with 2 wt% antioxidant B215 were mixed in a Hakke miniaturized internal mixer Rheomix 600 at a roll speed of 60 rpm for 12 min at 190 °C. The compounds were molded at 190 °C and 10 MPa into discs of 7.9 mm in diameter and 1.1 mm in thickness for rheological test and sheets for room temperature-resistance measurement. Samples containing coupling agent (10 wt% SMA) were also prepared as above.

Measurements

Dynamic rheological measurements were performed on an advance rheometric expanded system (ARES, Rheometrics, USA) in the mode of strain sweep with plate–plate grippers of 7.9 mm in diameter. The gap distance was kept about 1.0 mm for all tests. Strain sweeps from 0.1 to 100% were conducted at 3 rad/s and 170 °C. Two brass wires as electrodes were fixed to the torque transducer and the motor rods, respectively. The weights of the brass wires were too small to influence the rheological measurement. The in situ resistance change under shear strain was recorded using a computer controlled system based on a digital multimeter (Escort-3146A, Schmidt Scientific Taiwan Ltd., China) connecting to the brass wires. Illustration of the simultaneous measurement instrument is given in Scheme 1.

Thin sections, approximately 60–80 nm thick, of the composites were microtomed at room temperature for morphology observation using a JEOL JEM-1230 transmission electron microscopy (TEM) at an accelerating voltage of 120 kV.

A two-probe resistance measurement was carried out for determining resistivity (ρ) at room temperature, using a

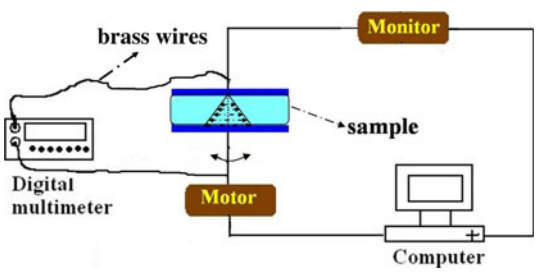

Scheme 1 Illustration of simultaneous measurement of dynamic moduli and resistance R

M890 B digital multimeter for resistance lower than $1.2 \times 10^8\ \Omega$ or using a high-resistance meter (ZC36; 10^{-14} A and $10^{17}\ \Omega$) for resistance higher than $1.2 \times 10^8\ \Omega$. The sheets (diameter 50 mm, thickness 1.2 mm) were used for high-resistance measurement. The sheets (length 35 mm, breadth 12 mm, thickness 1.2 mm) were used for low resistance measurement and two pieces of copper nets were mounted onto the opposite wide surfaces of the sheet to ensure good electric contact with the copper electrodes.

Results and discussions

Strain softening

Figure 1 shows dynamic storage modulus (G') and loss modulus (G'') as a function of strain (γ) for VGCF/PS composites. The significant increases of G' and G'' with increasing filler volume content (φ) indicate the reinforcement effect of VGCF. The pure matrix exhibits a linear viscoelastic regime up to about $\gamma = 30\%$. In contrast, G' and G'' of the composites begin to decrease at γ as low as 0.1% and there exists essentially no linearity regime. For the composites containing more than 8 vol.% VGCF, G' and G'' show a pronounced decrease at $\gamma < 10\%$, and an even more sharpened decrease at $\gamma > 30\%$, which has been seldom observed [10, 35].

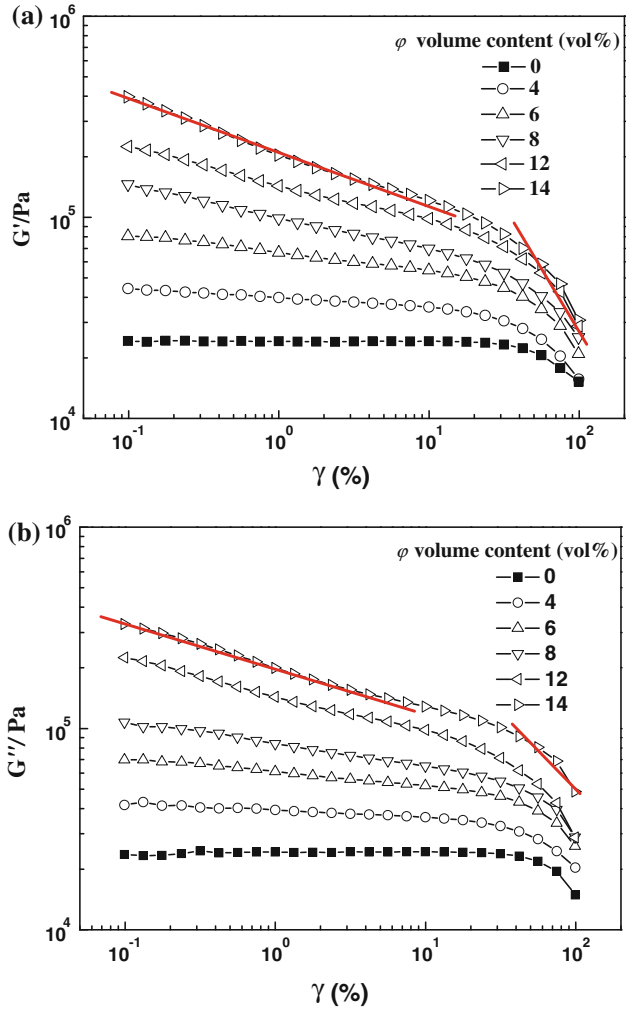

Fig. 1 Dynamic storage modulus G' (**a**) and loss modulus G'' (**b**) as function of strain γ at 170 °C for VGCF/PS composites with different VGCF volume fractions φ

It is accepted that reinforcement is related to the combinational contribution of the filler–filler and the filler–matrix interactions. Breakdown of these interactions and disentanglement of matrix macromolecules are considered to be responsible for strain softening. In general, their contributions are difficult to be distinguished. However, the filled polymers in high γ region exhibit viscoelasticity similar to that of the matrix, suggesting that molecular disentanglement is essential for the strain softening at $\gamma > 30\%$ [36]. Apart from molecular disentanglement at large strains, breakdown of the filler–filler or the filler–polymer interactions should be responsible for strain softening especially at low strains.

To examine the role of macromolecular disentanglement in strain softening of VGCF/PS composites, superposition of $G' \sim \gamma$ and $G'' \sim \gamma$ curves of filled samples on those of pure PS at the high strain region is conducted through vertical and horizontal shifting. Figure 2a and b shows the master curves of G' and G'' as a function of γ for the composites with different VGCF contents. Excellent superposition can be achieved at $\gamma > 30\%$, demonstrating the importance of macromolecular disentanglement for strain softening at large γ. Table 1 lists vertical shift factors $f_1(\varphi)$ and $f_2(\varphi)$ for G' and G'', respectively, as well as horizontal shift factor $A(\varphi)$. Both the vertical and horizontal shift factors are related to strain amplification effect originated from the presence of hard and much less deformable filler particle in soft and highly deformable matrix. The rigid filler particles do not contribute to the deformation and the global strain of the filled polymer is concentrated in the matrix [37] so that the local strain of the matrix must exceed the macroscopic strain. $A(\varphi)$ increases with φ, as shown in Fig. 3. Guth–Gold equation has been proposed to describe the relationship between $A(\varphi)$ and φ for asymmetric rod-like particle [38]

$$A(\varphi) = 1 + 0.67k\varphi + 1.62(k\varphi)^2 \quad (1)$$

Here, k is a shape factor defined as the length of the filler aggregate divided by its breadth. Equation 1 is applied to fit the data in Fig. 3 and the satisfactory fitting result with $k = 6.5$ is presented as a solid curve. Universal contribution of conventional filler to linear [39] and nonlinear viscoelasticity [36] of filled polymers has been

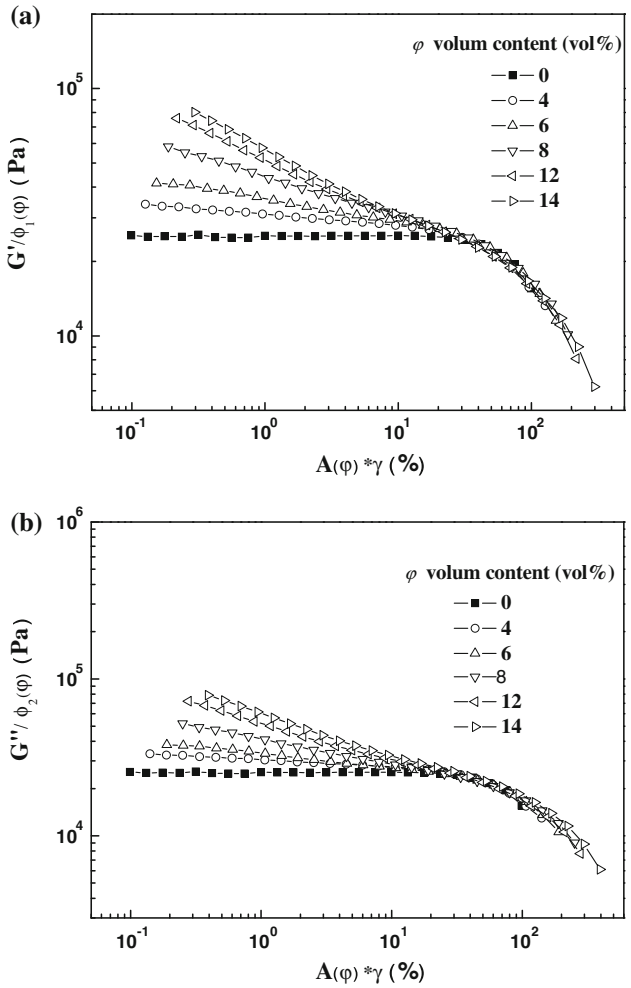

Fig. 2 Master curves of G' (**a**) and G'' (**b**) as a function of γ at 170 °C for VGCF/PS composites with different VGCF volume fractions φ

Table 1 Shifting parameters of strain-amplification effect for VGCF/PS composites with different VGCF contents φ

φ (vol.%)	$A(\varphi)$	$f_1(\varphi)$	$f_2(\varphi)$
4	1.3	1.3	1.4
6	1.6	1.9	2.0
8	1.9	2.5	2.6
12	2.3	3.6	3.4
14	3.0	4.8	4.5

explored by using the concept of strain amplification effect. For SiO_2 filled solution-polymerized styrene butadiene rubber [36], G' and loss tangent (tanδ) versus γ of the filled rubber can be superposed, respectively, on those of the matrix in a wide γ range, suggesting that the nonlinear viscoelasticity is mainly related to macromolecular disentanglement while SiO_2 only introduces a strain amplification effect. On the other hand, the $G' \sim \gamma$ and $G'' \sim \gamma$ curves of the VGCF/PS composites at $\gamma < 30\%$

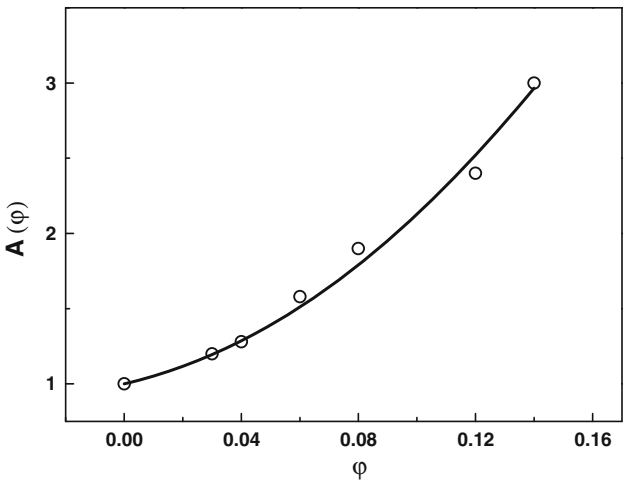

Fig. 3 $A(\varphi)$ as a function of φ for VGCF filled PS. *The solid curve* is drawn according to Eq. 1

could hardly be superposed onto the respective curves of pure PS. The deflection becomes more significant with increasing φ, implying that some filler-related structures are broken down under shear strains. In other words, breakdown of the filler–filler or the polymer–filler interactions may be responsible for the softening at strains below the onset of molecular disentanglement.

To confirm the speculation, coupling agent SMA was added in the composites containing 10 vol.% VGCF to weaken the filler–filler interactions as well as to strengthen the filler–matrix interactions [40]. Figure 4 shows TEM micrographs of 10 vol.% VGCF filled PS with 10 wt% SMA or without SMA. Addition of SMA promotes the dispersion of VGCF in the matrix and leads to a significant increment of interfiber distance (Fig. 4a) as compared to the case without SMA (Fig. 4b). Figure 5 shows influence of 10 wt% SMA on G' against γ for the composites. Addition of SMA can lower the G' value over the whole γ range and greatly weaken the strain softening effect in the low γ region. In fact, linear viscoelastic regime appears at $\gamma < 0.2\%$ in the composite containing 10 wt% SMA. However, influence of SMA on the Payne effect becomes inconspicuous gradually with increasing γ, especially in the molecular disentanglement regime. These results suggest that the filler dispersion controls the initial modulus and the nonlinear rheology at small strains. Both the reduction in filler–filler interactions and the increase in filler–matrix interactions may weaken the strain softening at small strains. Therefore, the strain softening at small strains may be associated to disruption of the filler–filler and the filler–matrix interactions. Ten-Brinke et al. [40] studied the dynamic rheological behaviors of silica–rubber composites at different strain amplitudes and found that the filler–filler interactions are particularly perceptible when deformations are small.

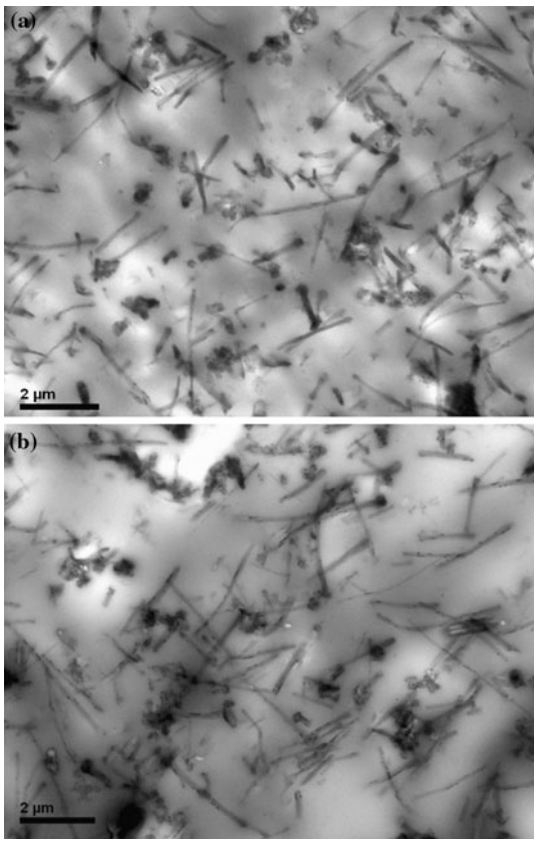

Fig. 4 TEM micrographs for 10 vol.% VGCF filled PS with 10 wt% SMA (**a**) and without SMA (**b**)

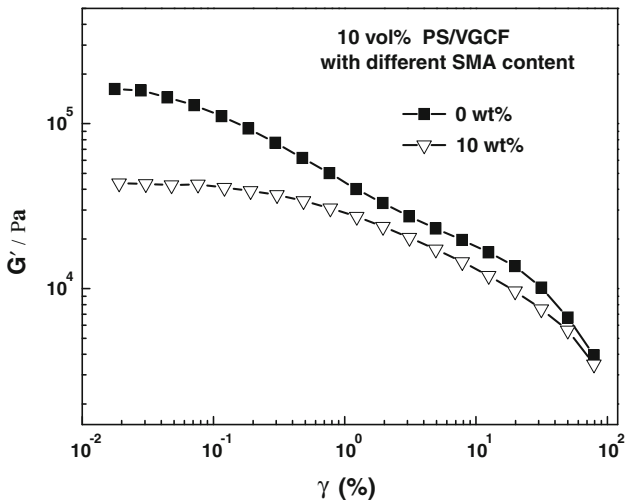

Fig. 5 G' as a function of strain γ at 170 °C for 10 vol.% VGCF filled PS with 10 wt% and without SMA

Evolution of filler structure under strain shear

Shearing filled polymers to a certain strain can disrupt the filler network, and as a result, influence the electrical conduction of the composites. Simultaneous measurements

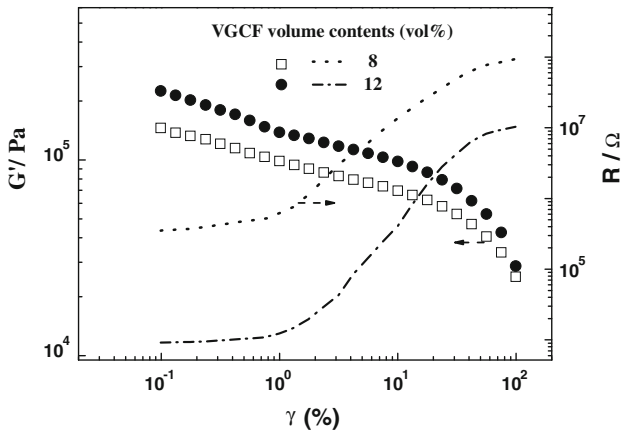

Fig. 6 G' and R as a function of γ for VGCF/PS composites at 3 rad/s at 170 °C

of R and G' as a function of γ would provide an effective evidence for filler network evolution. Figure 6 shows simultaneously measured R and G' as a function of γ for the composites containing 8 and 12 vol.% VGCF at 170 °C. R increases slightly at $\gamma < 1\%$ and sharply at large strains, which might be ascribed to the breakdown of direct fiber contacts and the substantial increase of interfiber distance [10, 35]. It seems that the filler network or the filler–filler interactions may be in breakdown–reformation equilibrium at very small strains [10, 41] while the breakdown process become dominative at a critical strain. The result well confirms that disruption of filler–filler interactions plays a vital role in strain softening of VGCF/PS composite. Disruption of the filler–filler interactions alone could not explain the nonlinear rheology at small strains and the marked modulus decline at small strains as shown in Fig. 1 should be partly attributed to breakdown of filler–matrix interactions in the vicinity of the filler inclusions, for example, desorption of PS chain from the filler surface during VGCF moving in the matrix.

TEM observation also gives some information about the filler-structure change due to shear action. Figure 7 shows morphologies for the composite containing 8 vol.% VGCF before and after being sheared at 50% strain amplitude for 10 min. It can be seen clearly that the fibers interconnect with each other and are randomly dispersed in the matrix before shearing while they orient along the shear direction. The fiber slippage and orientation may be accompanied by debonding of PS chain from the fiber surface, resulting in the reduction in fiber contacts and the increase in R with increasing γ.

Viscoelastic contribution of the filler phase

As aforementioned, VGCF filled PS exhibits marked strain softening with increasing strain amplitude, and the

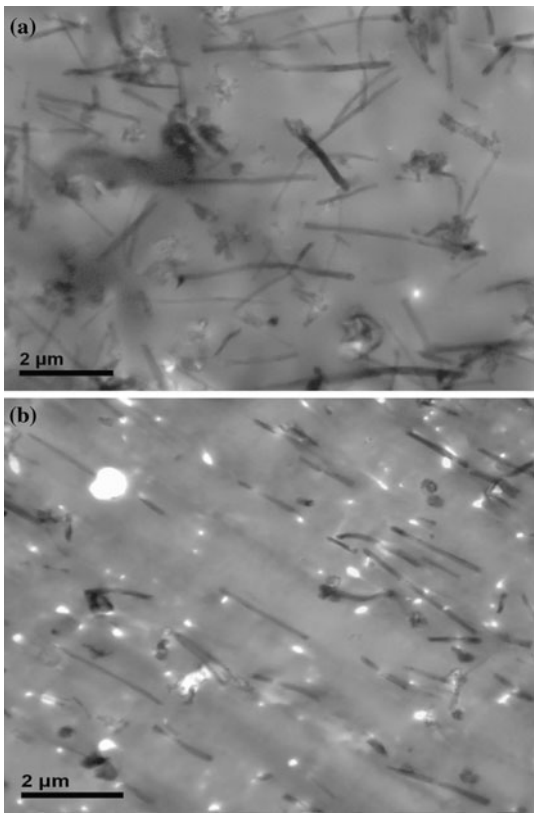

Fig. 7 TEM micrographs for 8 vol.% VGCF filled PS before (**a**) and after (**b**) being sheared at 50% strain amplitude for 10 min

amplitude of strain softening is very sensitive to filler concentration. Except for the strain amplification effect that enlarges the viscoelastic contribution of the matrix, the filler phase constructed from VGCF and the physically absorbed PS chains should also contribute to global viscoelasticity of the composites [42]. In a recently proposed two phase model, the global complex modulus of filled polymer can be divided into certain strain amplification effect and structural contribution of the filler phase. Complex modulus of filled polymer, $G^*_{c,(\gamma,\varphi)}$ can be expressed as

$$G^*_{c,(\gamma,\varphi)} = A(\varphi)G^*_{m,(A(\varphi)\gamma)} + G^*_{f,(\gamma,\varphi)} \quad (2)$$

Here, $G^*_{m,(A(\varphi)\gamma)}$ represents complex modulus of interstitial fluid between filler inclusions and $G^*_{f,(\gamma,\varphi)}$ is complex modulus of the filler phase. The values of $G^*_{c,(\gamma,\varphi)}$ and $G^*_{m,(A(\varphi)\gamma)}$ can be experimental determined.

Because it is impossible to measure static modulus of the filler phase in linear viscoelastic regime at extreme small strains, $\gamma = 0.1\%$ is selected for evaluating modulus of the filler phase in initial composites. As shown in Fig. 2, $G^*_{m,(A(\varphi)\gamma)}$ should not vary with increasing γ below 30%. So $G^*_{m,(A(\varphi)\gamma)}$ at 0.1% strain can be approximated as $G^*_{m,0.1\%}$ and the viscoelastic contribution of the initial structure of the filler phase can be estimated as

$$G'_{f,(0.1\%,\varphi)} = G'_{c,(0.1\%,\varphi)} - A(\varphi)G'_{m,0.1\%} \quad (3)$$

$$G''_{f,(0.1\%,\varphi)} = G''_{c,(0.1\%,j)} - A(\varphi)G''_{m,0.1\%} \quad (4)$$

Equations 3 and 4 allow estimating elastic and viscous moduli ($G'_{f,0.1\%}$ and $G''_{f,0.1\%}$) of the filler phase at 0.1% strain from those of the composite ($G'_{c,0.1\%}$ and $G''_{c,0.1\%}$) and the matrix ($G'_{m,0.1\%}$ and $G''_{m,0.1\%}$).

Electric conduction percolation may be related to viscoelasticity of the filler phase. Figure 8a shows percolation plots of volume resistance (ρ) at room temperature and elastic and viscous moduli ($G'_{c,0.1\%}$ and $G''_{c,0.1\%}$) at 170 °C as a function of $\varphi - \varphi_c$. According to classical percolation theory [43], ρ as a function of φ can be expressed as

$$\rho \sim (\varphi - \varphi_c)^{-\alpha} \quad (\varphi > \varphi_c) \quad (5)$$

The critical exponent α is determined as 1.41 ± 0.12, being in agreement with the value of 1.60 predicted in statistic percolation theories for three-dimensional systems [44, 45]. Rigidity percolation theories [46–53] are sometimes used to account for the critical growth of modulus of the composite at $\varphi > \varphi_c$.

$$G'_{c,(0.1\%,\varphi)} \sim G''_{c,(0.1\%,\varphi)} \sim (\varphi - \varphi_c)^{\beta} \quad (6)$$

The critical exponent β is determined as about 0.67 from slopes of both $G'_{c,0.1\%}$ and $G''_{c,0.1\%}$ against $\varphi - \varphi_c$, being close to the value of 0.70 in single-walled carbon nanotube/poly(methyl methacrylate) nanocomposite [54].

Figure 8b shows dynamic moduli for the composite and the filler phase at 0.1% strain as a function of φ in double-logarithmic plot. Both $G'_{f,0.1\%}$ and $G''_{f,0.1\%}$ increase linearly with increasing φ, following a scaling law predicted for cluster–cluster aggregation (CCA) model [43, 55, 56].

$$G'_{f,(0.1\%,\varphi)} \sim G''_{f,(0.1\%,\varphi)} \sim \varphi^x \quad (7)$$

Exponent $x \approx 2.51$ is determined from $G'_{f,0.1\%}$ and $G''_{f,0.1\%}$. On the other hand, the scaling law

$$G'_{c,(0.1\%,\varphi)} \sim G''_{c,(0.1\%,\varphi)} \sim \varphi^y \quad (8)$$

with $y \approx 1.80$ holds only at φ above percolation threshold $\varphi_c = 5.05$ vol.%.

Figure 8c shows ρ and relative moduli $G'_{f,0.1\%}/G'_{c,0.1\%}$ and $G''_{f,0.1\%}/G''_{c,0.1\%}$ as a function of φ. The plot indicates that the electrical conduction of the composites is directly connected with the structure of the VGCF phase. Relative moduli increase sharply at 2 vol.% $< \varphi <$ 8 vol.%, which is consistent with the sharp decay of ρ as a function of φ usually termed as percolation transition. The direct VGCF–VGCF contact allows establishing a conduction network,

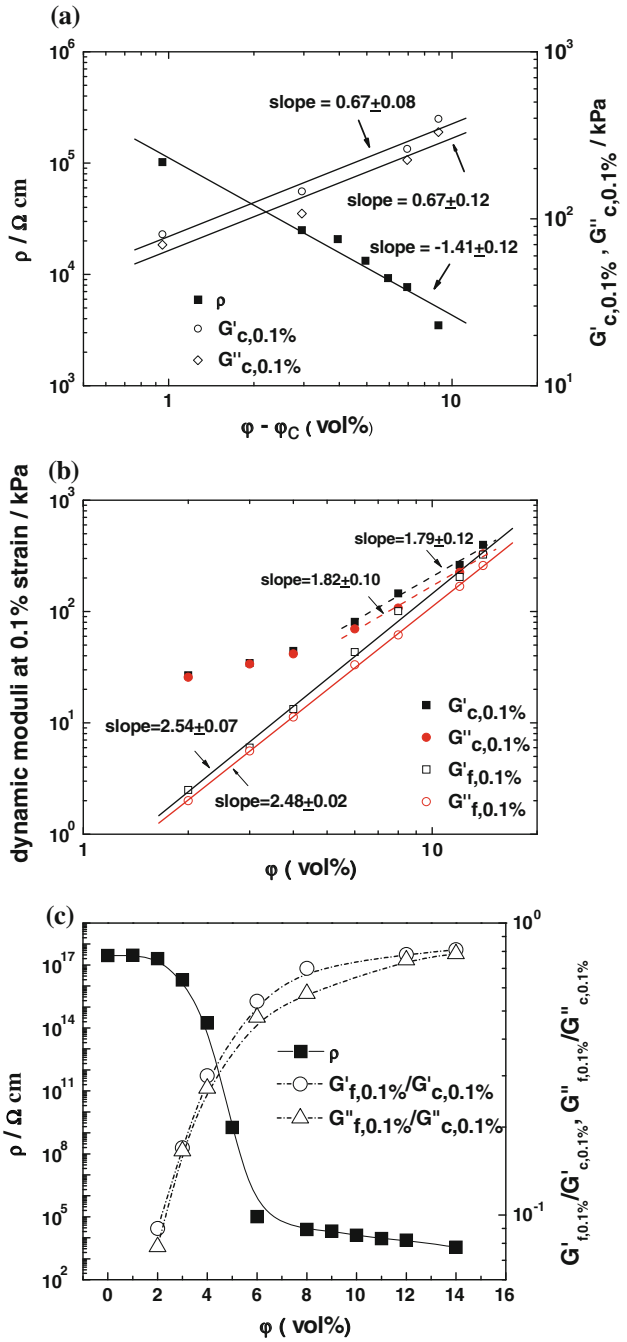

Fig. 8 **a** Volume resistivity ρ at room temperature and dynamic moduli $G'_{c,0.1\%}$ and $G''_{c,0.1\%}$ of composites at 170 °C as a function of $\varphi - \varphi_c$. **b** Dynamic moduli $G'_{c,0.1\%}$ and $G''_{c,0.1\%}$ of composites and $G'_{f,0.1\%}$ and $G''_{f,0.1\%}$ of the filler phase as a function of φ. **c** ρ and relative moduli $G'_{f,0.1\%}/G'_{c,0.1\%}$ and $G''_{f,0.1\%}/G''_{c,0.1\%}$ as a function of φ

resulting in the sharp electrical percolation transition. Apart from the role of VGCF in network, the matrix macromolecules must participate in the network formation through physical absorption on VGCF surface and bridging adjacent VGCF. This rheological network results in the fast increments of relative moduli of the filler phase with respect to the composites. At $\varphi > 8$ vol.%, both ρ and relative moduli level off gradually. The role of VGCF in reinforcement can be directly evaluated by the relative moduli $G'_{f,0.1\%}/G'_{c,0.1\%}$ and $G''_{f,0.1\%}/G''_{c,0.1\%}$ though these two parameters show slight difference at 6 vol.% $< \varphi <$ 12 vol.%.

Conclusion

The nonlinear viscoelasticity of VGCF/PS composites is associated with both chain disentanglements and disruption of filler–filler interactions depending on VGCF concentration and amplitude deformation. On the basis of the strain amplification concept, the strain softening region dominated by disentanglement can be defined for VGCF filled PS melts at large strains. Simultaneous measurement of R and dynamic moduli indicates that breakdown of the filler–filler or the polymer–filler interactions should be responsible for the Payne effect at strains below the onset of macromolecular disentanglement. The filler–filler interactions may be in breakdown–reformation equilibrium at extremely small strains while the breakdown process becomes dominative with increasing strain before onset of macromolecular disentanglement. Furthermore, reinforcement in filled polymer can be divided into the strain amplification effect and the structural contribution of the filler phase. Relative moduli $G'_{f,0.1\%}/G'_{c,0.1\%}$ and $G''_{f,0.1\%}/G''_{c,0.1\%}$, representing relative viscoelastic contribution of the filler phase with respect to the composite, show a percolation-like transition as a function of φ, which is in consistence with electric percolation transition.

Acknowledgement This work was supported by the National Natural Science Foundation of China (No. 50728302).

References

1. Hwang SJ, Joo YL, Lee SJ (2008) J Appl Polym Sci 110:1441
2. Kemal I, Whittle A, Burford R, Vodenitcharova T, Hoffman M (2009) Polymer 50:4066
3. Stojanovic D, Orlovic A, Markovic S, Radmilovic V, Uskokovic PS, Aleksic R (2009) J Mater Sci 44:6223. doi:10.1007/s10853-009-3842-8
4. Tamura K, Uno H, Yamada H, Umeyama K (2009) J Polym Sci B 47:583
5. Yilmaz MG, Unal H, Mimaroglu A (2008) Express Polym Lett 2:890
6. Harwood JAC, Payne AR (1966) J Appl Polym Sci 10:315
7. Payne AR (1965) J Appl Polym Sci 9:1073
8. Payne AR (1962) J Appl Polym Sci 6:57
9. Heinrich G, Kluppel M (2002) J Appl Polym Sci 160:1
10. Liu ZH, Song YH, Zhou JF, Zheng Q (2007) J Mater Sci 42:8757. doi:10.1007/s10853-007-1858-5
11. Zhu Z, Thompson T, Wang SQ, von Meerwall EV, Halasa A (2005) Macromolecules 38:8816

12. Witten TA, Rubinstein M, Colby RH (1993) J Phys II 3:367
13. Huber G, Vilgis TA (2002) Macromolecules 35:9204
14. Sternstein SS, Zhu AJ (2002) Macromolecules 35:7262
15. Malchev PG (2007) J Rheol 51:235
16. Cipriano BH, Kota AK, Gershon AL et al (2008) Polymer 49:4846
17. Yang S, Benitez R, Fuentes A, Lozano K (2007) Compos Sci Technol 67:1159
18. Ghose S, Watson KA, Working DC, Connell JW, Smith JG Jr, Sun YP (2008) Compos Sci Technol 68:1843
19. Dalmas F, Cavaille JY, Catherine G, Chazeau L, Dendievel R (2007) Compos Sci Technol 67:829
20. Al-Saleh MH, Sundararaj U (2009) Carbon 4:2
21. Berber S, Kwon YK, Tomanek D (2000) Phys Rev Lett 84:4613
22. Baughman R, Zakhidov A, De Heer W (2002) Science 297:787
23. Zeng J, Saltysiak B, Johnson WS, Schiraldi DA, Kumar S (2004) Compos Part B Eng 35:173
24. Tetsuya U, Anderson DP, Minus ML, Kumar S (2006) J Mater Sci 41:5851. doi:10.1007/s10853-006-0324-0
25. Salvetat JP, Bonard JM, Thomson NH, Kulik AJ, Forro L, Benoit W, Zuppiroli L (1999) Appl Phys A 69:255
26. Endo MKY, Hayashi T, Nishmura K, Matusita T, Miyashita KDM (2001) Carbon 39:1287
27. Ebbesen TW, Lezec HJ, Hiura H (1996) Nature 382:54
28. Ceccia S, Ferri D, Tabuani D, Maffettone PL (2008) Rheol Acta 47:425
29. Wang Y, Xu J, Bechtel S, Koelling K (2006) Rheol Acta 45:919
30. Schaefer DW, Zhao J, Dowty H, Alexanderc M, Orlerd EB (2008) Soft Matter 4:2071
31. Voet A, Cook FR (1968) Rubber Chem Technol 41:1207
32. Pan XD, Mckinley GH (1998) Langmuir 14:985
33. Liu ZH, Song YH, Shangguan YG, Zheng Q (2007) J Mater Sci 42:2903. doi:10.1007/s10853-007-1603-0
34. Liu ZH, Song YH, Shangguan YG, Zheng Q (2008) J Mater Sci 43:4828. doi:10.1007/s10853-008-2697-8
35. Leboeuf M, Ghamri N, Brule B, Coupez T, Vergnes B (2008) Rheol Acta 47:201
36. Sun J, Song YH, Zheng Q, Tan H, Yu J, Li H (2007) J Polym Sci B 45:2594
37. Osman M, Atallah A, Schweizer T, Ottinger HC (2004) J Rheol 1167
38. Mullins L, Tobin NR (1965) J Appl Polym Sci 9:2993
39. Song YH, Zheng Q, Cao Q (2009) J Rheol 53:1379
40. Ten-Brinke JW, Debnath SC, Reuvekamp LAEM, Noordermeer JWM (2003) Compos Sci Technol 63:1165
41. Lv RH, Xu WF, Na B, Chen BB (2008) J Macromol Sci B 47:774
42. Song YH, Zheng Q (2010) Polymer 51:3262
43. Klüppel M (2003) Adv Polym Sci 164:1
44. Medalia AI (1986) Rubber Chem Technol 59:432
45. Kirkpatrick S (1973) Rev Mod Phys 45:574
46. Prasad V, Trappe V, Dinsmore AD, Segre PN, Cipelletti L, Weitz DA (2003) Faraday Discuss 123:1
47. Trappe V, Weitz DA (2000) Phys Rev Lett 85:449
48. Romeo G, Filippone G, Fernandez-Nieves A, Russo P, Acierno D (2008) Rheol Acta 47:989
49. Kantor Y, Webman I (1984) Phys Rev Lett 52:1891
50. Feng SC, Sahimi M (1985) Phys Rev B 31:1671
51. Arbabi S, Sahimi M (1988) Phys Rev B 38:7173
52. Sahimi M, Arbabi S (1993) Phys Rev B 47:703
53. Benguigui L (1986) Phys Rev B 34:8176
54. Du F, Scogna RC, Zhou W, Brand S, Fischer JE, Winey KI (2004) Macromolecules 37:9048
55. Potanin AA, Russel WW (1996) Phys Rev E 53:3702
56. Potanin AA, Derooij R, Vandenende D, Mellema J (1995) J Chem Phys 102:5845